Hindawi
Journal of Robotics
Volume 2018, Article ID 6756027, 12 pages
https://doi.org/10.1155/2018/6756027

Research Article

Biomechanic and Energetic Effects of a Quasi-Passive Artificial Gastrocnemius on Transtibial Amputee Gait

Michael F. Eilenberg, Ken Endo, and Hugh Herr

Biomechatronics Group, MIT Media Lab, Massachusetts Institute of Technology, Cambridge, MA 02139, USA

Correspondence should be addressed to Hugh Herr; hherr@media.mit.edu

Received 15 April 2017; Revised 16 August 2017; Accepted 25 September 2017; Published 1 March 2018

Academic Editor: Kazuo Kiguchi

State-of-the-art transtibial prostheses provide only ankle joint actuation and thus do not provide the biarticular function of the amputated gastrocnemius muscle. We develop a prosthesis that actuates both knee and ankle joints and then evaluate the incremental effects of this prosthesis as compared to ankle actuation alone. The prosthesis employs a quasi-passive clutched-spring knee orthosis, approximating the largely isometric behavior of the biological gastrocnemius, and utilizes a commercial powered ankle-foot prosthesis for ankle joint functionality. Two participants with unilateral transtibial amputation walk with this prosthesis on an instrumented treadmill, while motion, force, and metabolic data are collected. Data are analyzed to determine differences between the biarticular condition with the activation of the knee orthosis and the monoarticular condition with the orthosis behaving as a free-joint. As hypothesized, the biarticular system is shown to reduce both affected-side knee and hip moment impulse and positive mechanical work in both participants during the late stance knee flexion phase of walking, compared to the monoarticular condition. The metabolic cost of walking is also reduced for both participants. These very preliminary results suggest that biarticular functionality may provide benefits beyond even those of the most advanced monoarticular prostheses.

1. Introduction

The loss of a leg below the knee can have a formidable impact on one's quality of life [1–3]. The widespread, passive ankle-foot prostheses on the market today provide only a rudimentary approximation to the function of a human ankle joint [4, 5]. Instead of providing net mechanical work to the wearer during walking, these passive devices act at best in a spring-like manner; they can only provide as much mechanical energy return as is provided to them by the wearer, and they do not provide the articulation normally seen in the biological ankle-foot complex during walking. As evidence of this technological limitation, transtibial amputees display a variety of pathological features of their walking gaits. Specifically, transtibial amputees naturally select a 30–40% slower walking speed than those without amputation, and when walking at the same pace as a nonamputee, these amputees require 20–30% more metabolic power than their nonamputee counterparts [4, 6–8]. Further, these amputees exhibit increased levels of hip positive power during late stance phase. This increased hip power may be a compensatory response to lack of calf muscle function and could contribute to the aforementioned increase in metabolism while walking [4].

In the last several years, robotic advances in prosthetic technology have led to the introduction of powered ankle-foot prostheses (EmPower, BionX Medical Technologies, Inc., Bedford, MA), which, unlike the passive conventional devices, provide levels of mechanical work comparable to those provided by the human ankle-foot complex. As a result of this functional improvement, many of the aforementioned gait pathologies have been drastically reduced; amputees using the powered prostheses have preferred walking speed, metabolic cost at a given speed, and contralateral limb impacts that are not significantly different from those of nonamputees [9, 10]. These improvements are thought to stem from the propulsive net mechanical work provided by these devices to the wearer [9], as this propulsion helps to

redirect the center-of-mass, thereby reducing collisions of the contralateral limb [11–14]. This ankle propulsion may also assist swing-initiation of the affected-side limb [15–18].

These new prosthetic devices are, however, limited to emulating the function of the ankle-foot complex alone and consequently cannot restore the full function of the powerful gastrocnemius muscle. The gastrocnemius provides not only a plantar flexion moment at the ankle, but also a flexion moment at the knee. Without the knee-flexing function, compensatory mechanisms are required. Indeed, transtibial amputees exhibit higher hamstring muscle activity during level-ground walking than nonamputees [19], possibly as an attempt to stabilize or flex the knee in place of the nonfunctional gastrocnemius muscle. This higher muscle activity is still apparent when amputees walk with the powered ankle-foot prostheses, indicating that a monoarticular intervention at only the ankle-foot complex may not be sufficient to restore biological function. It is possible that this pathological muscle activity has detrimental effects on amputee gait. However, little work has been done to develop devices for restoring this missing gastrocnemius functionality.

Since those with transtibial amputation maintain their biological knee joints, a direct assistance of these joints requires the use of an exoskeletal device such as an orthosis that provides assistance in parallel to the existing joint. A variety of robotic orthoses have been developed to assist human knee joints for locomotion. Many of these devices utilize active components such as electric motors [20–22] or pneumatic actuators [23–26], but these elements tend to require a large power source or otherwise require off-board tethered actuation, limiting the scope of their applicability. Alternatively, some researchers have developed quasi-passive knee exoskeletons that do not provide net mechanical power to the wearer but instead require at most the minimal input power to operate the electronics and mechanical components [27–30]. In one such study, a spring-loaded, custom toothed clutch was designed for assisting extension moment during human running [29]. This device locked to support the knees of nonamputee participants during the stance phase and unlocked to be a free joint during the swing phase. Using this quasi-passive device, large knee moments of 190 Nm could be supported with an exoskeletal joint weighing only 710 grams. This, and other exoskeletons have been built to assist with knee extension in nonamputees, but no such devices to date have been built for knee flexion assistance, particularly for the gastrocnemius, in those with transtibial amputation.

In order to develop an assistive device for the gastrocnemius, it is important to first understand how this muscle functions. In vivo ultrasonography shows that the gastrocnemius muscle fascicle length is largely isometric during the early and mid-stance phases of level-ground walking [31], indicating that the passive tissues such as tendons are responsible for much of the power delivery from the gastrocnemius. Hence, the gastrocnemius may be approximated by a clutched spring, with the spring representing the compliant tendinous structures, and the clutch representing the isometrically acting muscle fibers. Indeed, a model of human gait by Endo and Herr with only spring-clutch structures at the knee joint was able to achieve human-like metabolic economy, while capturing the dominant kinetic features of human walking [32–34]. It is therefore possible that a physical clutch in series with a spring can provide much of the missing knee function of the gastrocnemius in transtibial amputees.

Researchers have begun to study the effects of a robotic device at the affected-side knee to provide the knee flexion moment of the missing gastrocnemius. In the first such study [35], a quasi-passive knee orthosis, dubbed an artificial gastrocnemius (AG) was built, based on the spring-clutch representation of the gastrocnemius in the aforementioned Endo-Herr model. The AG was physically realized as clutchable rotary spring at the orthosis knee joint. Two copies of this AG, worn along with a powered-ankle-foot prosthesis (PAFP), was tested on both legs of one bilateral transtibial amputee, with promising results: the amputee's metabolic energy expenditure was reduced with the AG-PAFP condition, compared to the amputee walking at the same speed with only conventional leaf-spring-type ankle-foot prostheses. However, since the PAFP was not tested independently of the AG, it is not clear what incremental effects the AG had over the PAFP alone. A need, therefore, exists to evaluate the incremental biomechanical and metabolic effects of the AG.

In this study, we design and evaluate a new version of the AG unit, based on the exoskeletal knee clutch design [29]. We evaluate the effects of this new AG-PAFP on the walking gait of transtibial amputees. We focus on the late stance knee flexion phase of walking, during which the knee flexes to prepare for the swing phase, so to detect improvements on the pathologies thought to be most likely affected by the lack of calf muscle function [4]. We expect that the energy stored in the spring of the AG early in the gait cycle will be returned during late stance knee flexion to replace positive muscle work. Specifically, we hypothesize that including a clutched-spring AG at the affected-side knee joint of transtibial amputees in conjunction with a PAFP will reduce both biological flexion moment impulse and positive mechanical work of the affected-side knee and hip joints during late stance knee flexion, as compared to the same conditions with only the PAFP. We further hypothesize that these changes will provide a corresponding reduction in metabolic cost of walking. We expect that this metabolic reduction will stem from reduced joints moments and net work in the affected knee and hip joints. We evaluate these hypotheses by analyzing the kinematics, kinetics, and metabolism of two transtibial amputees walking with the AG-PAFP combination on an instrumented treadmill. We compare these data between the two conditions where the AG is active versus acting as a free-joint.

2. Methods

Two devices were used for the intervention in this study. A powered ankle-foot prosthesis provided ankle function in the sagittal plane, and a quasi-passive artificial gastrocnemius (AG), that was a clutched-spring joint, was mounted on a knee orthosis on the affected-side knee. Together, these two devices represented a biarticular transtibial prosthesis that could actuate both joints independently.

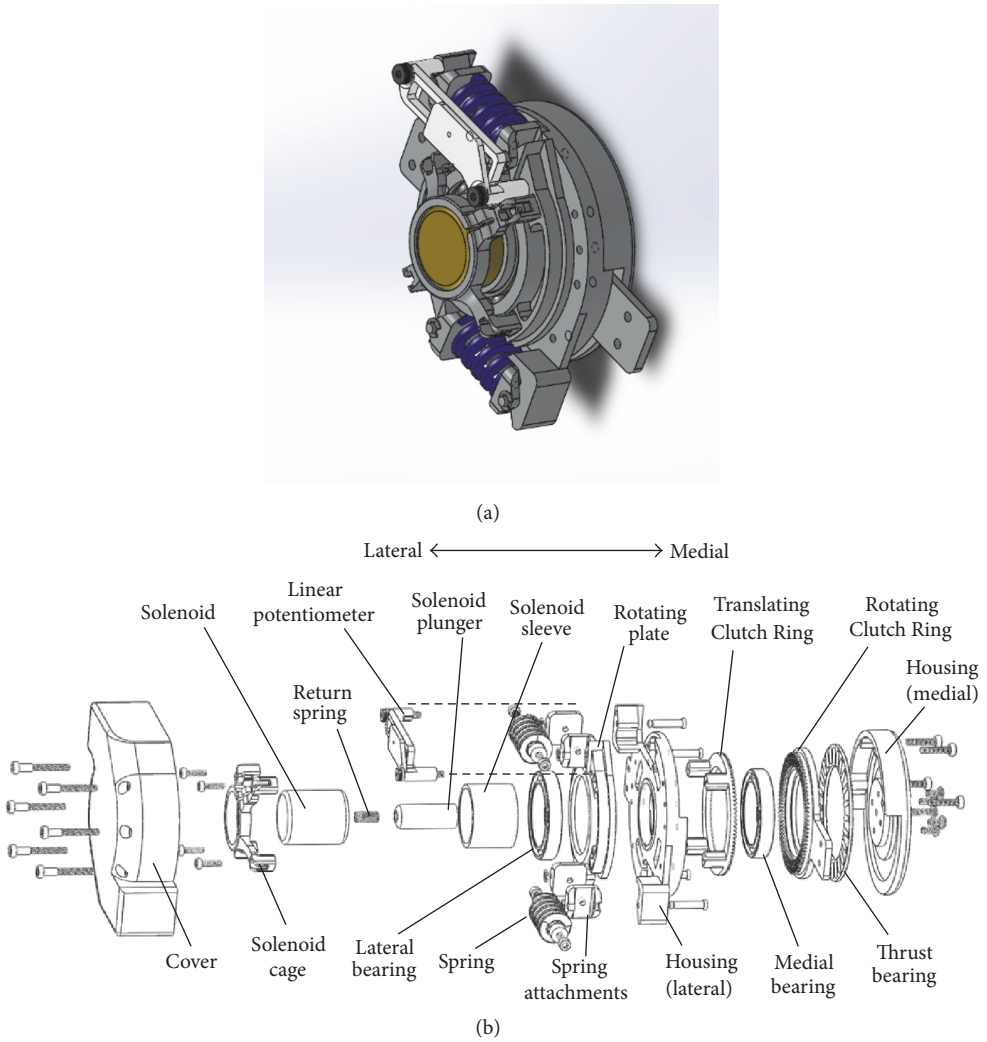

Figure 1: Joint mechanism of the quasi-passive artificial gastrocnemius. The exploded view of the joint design (b) is shown along with a rendering of the assembled joint without the cover (a). The *Housing* was attached to the proximal part of the orthosis, and the *Rotating Clutch Ring* attached to the distal part of the orthosis.

2.1. Powered Ankle-Foot Prosthesis. An EmPower powered ankle-foot prosthesis (BionX, Bedford, MA) was used as the prosthesis for all clinical trials. This prosthesis had the capability of providing positive net power at levels comparable to the human ankle-foot complex [9]. At the core of the prosthesis was a series elastic actuator, comprising a brushless DC motor, ball screw, and carbon fiber leaf spring. For dorsiflexion angles, a rigid hard-stop engaged, both to reduce the torque required by the motor in dorsiflexion and to act as a safety feature in the event of a power failure. The total mass of the prosthesis and battery was 1.8 kg.

The prosthesis controller employed a positive force feedback strategy that served to approximate the biological muscle dynamics and neural reflexes. A wireless communication link enabled real-time tuning of the control parameters.

2.2. Clutch-Spring Joint. The AG, shown in Figure 2, was a knee orthosis, comprising a pair of polycentric hinges that connected a thigh cuff to an 1/8″-thick aluminum bracket made of aluminum sheet stock (6061-T6). The bracket connected to the base of a participant's socket, between the prosthetic pylon attachment and the socket. The proximal side of the brace was strapped to the participant's thigh as a typical knee orthosis. A custom, dog-tooth rotary clutch spring with series compliance was attached lateral to the knee, in parallel with the hinges.

This clutch-spring joint was based on a previous design [29] but had the addition of series compliance and reversed the direction of the clutch teeth so that the teeth engaged to provide a knee flexion moment, rather than an extension moment to the wearer. In addition, our device lacked a planetary gear train that was present in the previous work. The machined clutch components were made of 6061-T6 aluminum alloy and included two rings of dog teeth, brought together by the action of a solenoid (LT8x9, Guardian Electric, Woodstock IL). As in Figure 1, the clutch controlled the relative rotation of the *Housing* to the *Rotating Clutch Ring*. A solenoid was built into the middle of the joint and translated

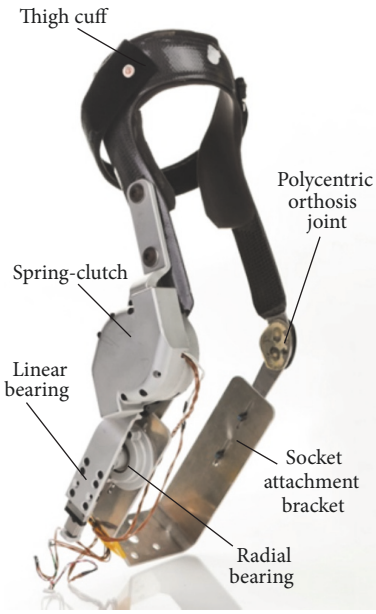

Figure 2: Quasi-passive artificial gastrocnemius (photo credit: Chris Conti Photography).

in the medial-lateral direction under action of its actuation power and a return spring. When the solenoid was energized, the *Translating Clutch Ring was engaged with the Rotating Clutch Ring*. The *Translating Clutch Ring* constrained the rotation of the *Rotating Plate* that, in turn, was connected to the *Housing* through two tangential linear compression springs. Thus, when the solenoid was energized, the *Housing* was coupled to the *Rotating Clutch Ring* through these springs. When the solenoid was inactive, the return spring separated the *Translating Clutch Ring* from the *Rotating Clutch Ring* and, hence, they were then free to rotate with respect to each other. The return spring stiffness was chosen experimentally so that when the clutch developed more than 0.5 Nm of torque, the tooth friction prevented the two rings from separating. This tooth-binding effect acted as a safety mechanism and was included as a part of the control algorithm, as described in Section 2.8. This aforementioned friction maintained the clutch in a clutched state until the torque level dropped back to the safe value of 0.5 Nm. As a result, the bulk of the stored spring energy could only be released gradually into the wearer's leg, rather than suddenly into the mechanism.

The *Housing* of the clutch was bolted to the thigh cuff of the knee orthosis. The *Rotating Clutch Ring* connected to a distal output link with a linear ball bearing and radial ball bearing, acting in series. These bearings accommodated for the kinematic difference between the polycentric hinges of the orthosis and the single-axis rotation of the clutch joint. Thus, only forces tending to flex or extend the joint could be transmitted through this set of bearings.

2.3. Sensing. The AG had onboard sensing for use in the control algorithm. Knee angle of the AG was measured using a 10 kOhm rotary potentiometer. Knee moment provided by the spring-clutch element to the wearer was estimated by measuring the deflection of one of the two identical tangential springs with an 8 kOhm linear potentiometer. The voltage output from the potentiometer was scaled with an experimentally determined gain to provide an estimate of torque applied by the AG to the wearer. This gain was found by applying various tangential forces to the distal end of the brace using a force gauge (gauge moment arm = 28 cm), while the clutch was engaged. With this force and the known moment arm of the gauge, the applied knee moment was computed and compared to voltage readings from the linear potentiometer to achieve a scaling factor for conversion from voltage to Nm/rad. The resulting measured spring-clutch knee torque reading is subsequently referred to as the AG knee moment. A similar calibration procedure was performed using the AG angle-sensing rotary potentiometer and an infrared camera system (model T40s, Vicon Motion Systems Ltc, Oxford, UK). In this calibration procedure, reflective markers were placed on the center of the joint and on the distal and proximal ends of the orthosis. Marker-based joint angle was computed by obtaining the relative angles of lines connecting the distal and proximal markers to the joint center marker. These angles were then compared to voltage readings from the angle-sensing potentiometer. Prosthesis-side ground contact was detected using a resistive pressure sole footswitch (model: FSW, B&L Engineering, Santa Ana, CA), inserted into the shoe between the prosthetic foot and the insole.

2.4. Failure Analysis. Unlike the titanium toothed rings in the exoskeletal clutch [29], the clutch in the present study was made from aluminum. Thus, it was necessary to reevaluate the load-bearing limits of the teeth. Finite element analysis (FEA) was performed using Solidworks (DS Solidworks Corp, Waltham, MA) to ensure this clutch could support the required knee moments. Tangential loads were simulated symmetrically on the tips of all teeth to simulate worst-case loading scenario.

2.5. Modeling and Spring Stiffness Selection. The selection of the spring constants for the tangential springs allowed for the control of rotary stiffness of the clutch-spring element. It was desirable for the stiffness of the clutch-spring joint to be such that the spring-clutch behavior of the artificial gastrocnemius would most closely reproduce the gastrocnemius muscle behavior of a healthy gastrocnemius. To this end, walking data from healthy nonamputees was fed as input to a modified version of the Endo-Herr sagittal-plane human leg model [32–34] during the development of the artificial gastrocnemius in [35].

2.6. Control. The quasi-passive artificial gastrocnemius produced no positive net mechanical work to the wearer but still required a control system to determine the appropriate times to engage and disengage the clutch. This controller took knee joint angle and stance information as input and engaged the clutch appropriately through each gait cycle. The clutch was controlled to engage at maximum stance knee flexion angle, enabling the spring to store energy during the subsequent

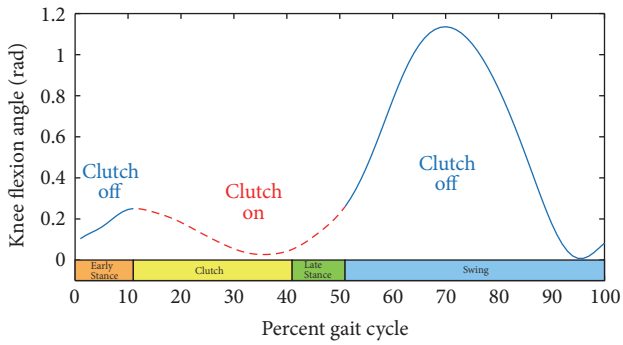

FIGURE 3: Example action of the clutch engagement. A typical knee flexion angle profile is shown for level-ground walking. The dashed red section indicates the region in the gait cycle when the clutch in the AG would be engaged. Colored bars show the sequence of intended finite-state-machine state transitions.

knee extension and flexion into swing phase, as shown in Figure 3.

2.7. Control Electronics. The computer platform for controlling the AG was a commercial single-board computer (model: Raspberry Pi Version B, Raspberry Pi Foundation, Cambridgeshire, UK). The computer was equipped with an 800 MHz ARM11 processor, 512 MB SDRAM, with Linux Debian. The system was powered by a 6-cell lithium polymer battery (nominal voltage of 22.2 V).

2.8. Control Algorithm. High-level control was implemented using a finite state machine, implemented in Python. The gait cycle was divided into four states, shown in Figure 4: (1) *Swing*; (2) *Early Stance*; (3) *Clutched*; and (4) *Late Stance*.

The *Swing* state was triggered from any other state when the affected-side foot left the ground, as detected by a drop in footswitch signal, FSW, to less than a fraction, foot_{SW} of the maximum possible signal. During *Swing*, the clutch was disabled, allowing the knee to swing freely.

The *Early Stance* state was triggered from the *Swing* state at foot contact of the affected-side with the ground, defined as FSW increasing to the stance threshold, foot_{ST}, provided that the time elapsed in the current state, t_{state}, was at least the minimum time required for the *Swing* state, t_{swing}. During the *Early Stance* state, the clutch was disabled, and the controller monitored the knee angle of the brace for maximum stance knee flexion, at which point the *Clutched* state would be engaged. A least squares algorithm, similar to the one used previously [29], continually predicted the time remaining before maximum knee flexion angle. This prediction provided time to initiate the engagement of the clutch, so that the clutch would be fully engaged as close as possible to the time of maximum knee flexion. In addition to this knee flexion detection algorithm, two safety features were in place to ensure that the motions detected were resulting from a walking gait. The *Clutched* state could only be enabled if the following two conditions were also met: (1) the knee was flexed a minimum angle of θ_{ES} from the angle at heel strike, θ_{HS}; (2) the maximum knee flexion angular velocity, $\dot{\theta}_{\text{max}}$, measured during the *Early Stance* state was at least $\dot{\theta}_{\text{ES}}$. The values θ_{ES} and $\dot{\theta}_{\text{ES}}$ were experimentally determined during early testing as the lowest values that successfully prevented false-triggering of the *Clutched* state outside of a steady, level-ground walking gait (Table 1).

The *Clutched* state served to activate the clutch near the maximum knee flexion during stance phase of walking. This state was activated when the following criteria were met: (1) the maximum stance flexion angle was predicted to occur within the time t_{delay} of the current time, (2) the knee angle was flexed more than a threshold, θ_{ES}, and (3) the maximum knee flexion angular velocity, $\dot{\theta}$, during the *Early Stance* state exceeded a threshold $\dot{\theta}_{\text{ES}}$. Conditions (2) and (3) were used to differentiate a walking gait with slow, nongait motions, the latter of which did not warrant activation of the clutch.

The *Late Stance* state served to turn off the clutch after it engaged. Once the clutch spring began to develop force, the clutch teeth would bind, preventing the clutch from disengaging until the spring force dropped sufficiently. Therefore, the clutch solenoid was deactivated by entering the *Late Stance* state when the time elapsed in the *Clutched* state, t_{state}, exceeded the clutch timeout threshold, t_{cl}.

In order to maximize spring energy storage and return, it was desirable to engage the clutch as near as possible to the moment of peak knee flexion in the *Early Stance* state. In fact, the clutch solenoid needed to be engaged slightly before the desired clutching time, as to account for the time required to close the gap between the two sets of clutch teeth. To achieve the necessary prediction of peak stance flexion, a look-ahead algorithm was used.

First, the knee angle during the *Late Stance* state was approximated as parabolic, given this assumption, the location of the vertex of the parabola may be found by performing a linear fit to the knee angular velocity data, via running sums, and solving for the zero-crossing. The algorithm used here was similar to one described by [29]. However, the earlier algorithm assumed a fixed time step that was not applicable with the system in this study, as the computer platform was not a truly real-time system. Hence, the algorithm proposed here did not presume a fixed time step.

The parameter $\boldsymbol{\beta} = [\beta_0 \;\; \beta_1]^T$ that minimizes the error in the least squares sense of linear model $\hat{y}(t) = \beta_0 + \beta_1 x(t)$ to time-series data $(x(t), y(t))$ is

$$\boldsymbol{\beta} = \left(\mathbf{X}^T\mathbf{X}\right)^{-1}\mathbf{X}^T\mathbf{y}, \tag{1}$$

where the matrix $\mathbf{X}$ has elements

$$X_{i,j} = \frac{\partial \hat{\mathbf{y}}}{\partial \beta_j} = \begin{cases} 1, & j = 0 \\ x_i, & j = 1 \end{cases} \tag{2}$$

and x_i is the ith element in the discretely sampled $x(t)$ vector. Expanding (1) yields

$$\boldsymbol{\beta} = \frac{\begin{bmatrix} \sum x_i^2 \sum y_i + \sum x_i \sum x_i y_i \\ \sum x_i \sum y_i + W \sum x_i y_i \end{bmatrix}}{W \sum x_i^2 - \left(\sum x_i\right)^2}, \tag{3}$$

Table 1: Parameter values for the AG controller.

Parameter	Description	Value
foot_{ST}	Footswitch threshold for entering the *Early Stance* state; fraction of the maximum possible value	0.2
foot_{SW}	Footswitch threshold for entering the *Swing* state	0.15
t_{swing}	Minimum time in the *Swing* state before it is possible to exit *Swing*	200 ms
θ_{ES}	Minimum knee flexion angle (rad) during the *Early Stance* state before the clutch can be engaged	0.087 rad
$\dot{\theta}_{\text{ES}}$	Minimum knee flexion angular velocity that must be observed during the *Early Stance* state before the clutch can be engaged	1.2 rad/s
t_{delay}	Delay time required between activation of the solenoid and the full engagement of the clutch	50 ms
t_{cl}	Maximum time to energize the solenoid	400 ms

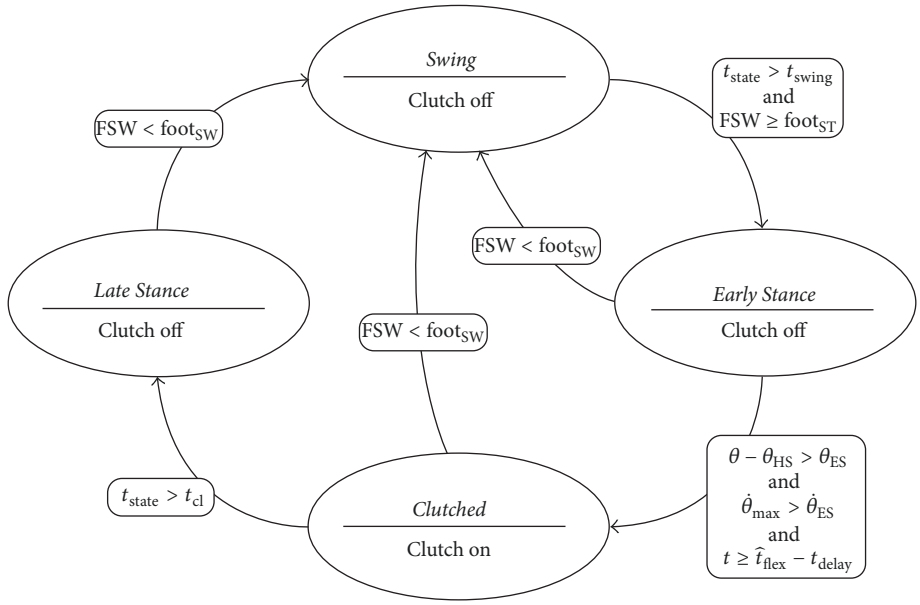

Figure 4: Finite state machine for the quasi-passive artificial gastrocnemius.

where all summations in (3) span i from 1 to W. For the task of estimating the angular velocity over time, the values of x_i were timestamps, and the values of y_i were knee angular velocity values. For the window of size W, the most recent W values of x and y were maintained in a queue. At each new timestep, the oldest values of x and y were popped from the queue, while the current x and y values were added to the queue, maintaining the 0th element as the first in the queue. This method allowed the sums to be updated each timestep without needing to store all values of the computed sums. Finally, the estimated time of the angular velocity zero-crossing was $\hat{t}_{\text{flex}} = -\beta_0/\beta_1$. It was found experimentally that the minimum error in clutching time between the initiation of the development of clutch torque and the peak knee flexion angle occurred when the clutch was engaged 50 ms prior to the predicted maximum knee angle. As a result, the time delay parameter, t_{delay}, was set to 50 ms.

2.9. Experimental Protocol. Two participants with below-knee amputation were involved in this study (Table 2). Both participants had right-side unilateral amputation and were of generally good health. The clinical evaluation was conducted at MIT (Cambridge, MA) and was approved by MIT's Committee on the Use of Humans as Experimental Subjects (COUHES). Each participant provided written, informed consent that was obtained before data collection was initiated.

Table 2: Amputee participant body parameters.

	Height (cm)	Weight (kg)
Subject 1	180	93
Subject 2	193	94

An infrared camera system (model T40s, Vicon Motion Systems Ltc, Oxford, UK) was used to track the three-dimensional motion, recorded at 100 Hz, of reflective markers, placed at 47 anatomical locations on the participants' bodies, based on the Helen Hayes marker model. Ground reactions forces and center of pressure locations were measured using a dual-belt instrumented treadmill (Bertec Corporation, Columbus, OH) with a sampling rate of 1 kHz. The net metabolic cost of walking during each condition was estimated using standard open-circuit gas exchange techniques (model: K4b2, COSMED, Rome, Italy).

At the beginning of each session, the participant was asked to don the powered prosthesis in place of their conventional prosthesis. The knee orthosis of the AG was then affixed to the prosthesis and donned by the participant.

For each participant, the prosthesis controller's power setting was adjusted using the commercial tuning app as the participant walked over a treadmill at 1.25 m/s so as to achieve net work from the prosthesis per step that was within one standard deviation of the mean for nonamputees walking at the same walking speed [36]. It was verified that the level of prosthesis net work remained within the desired range for both walking conditions for a given participant (0.045 to 0.16 J/kg) and that this level of net work stayed reasonably consistent across walking conditions for each participant.

A short time period of approximately 15 minutes was given to ensure that both the prosthesis and the artificial gastrocnemius orthosis were functioning properly. This acclimatization was evaluated by verifying that the clutch was engaging and disengaging at appropriate points in the gait cycle (as in Figure 3) and that the PAFP net mechanical work was reasonable as compared to biological values.

Both the powered prosthesis and artificial gastrocnemius were worn for all trials. The participants were asked to perform one standing trial to measure standing metabolism. Walking trials were performed on the treadmill at a speed of 1.25 m/s.

Two walking conditions were tested: (1) a baseline condition (*Baseline*) in which the AG acted as a free-joint at the knee with the spring-clutch disabled, and (2) an active condition (*Active*), in which the AG was controlled as a clutched spring at the knee with the described control algorithm. For both conditions, the powered ankle-foot prosthesis was active. The *Baseline* condition represented a monoarticular transtibial prosthesis, as the knee joint was a free-joint when the clutch was inactive. Yet the mass distribution of the device was identical to the *Active* condition. Thus, a direct comparison could be made to determine the incremental effects of the clutched-spring knee joint.

2.10. Data Processing. Fourth-order Butterworth filters were used to filter the marker position and ground reaction force data with 6 Hz and 25 Hz cutoff frequencies, respectively. The marker and force data were postprocessed through the SIMM (Musculographics Inc., Evanston, IL) inverse dynamics module to produce total joint moments and angles in three dimensions. However, only sagittal-plane dynamics were considered. Affected-side biological knee moment contribution was computed by subtracting the AG knee moment from the total knee moment estimated from the SIMM-based inverse dynamics.

Gait events were determined using vertical ground reaction force data from the embedded force plates. Approximate event timing was found by determining the times when the force increased beyond a 40 N threshold. Exact heel strike and toe-off times were found by progressing backward and forward in time, respectively, until the force value dropped to zero. Data were then cut to gait cycles based on heel strike times and resampled to 101 points. Gait cycles were discarded for the beginning and end of each trial, during the speed transients of the treadmill. Gait cycles in which the stride times were below 0.7 seconds or above 1.3 seconds or in which a foot crossed the midline of the treadmill were also discarded.

Table 3: Mechanical design parameters of the artificial gastrocnemius joint.

Parameter	Value
Maximum torque (Nm)	890
Torque sensor scale factor (Nm/V)	825
Number of teeth	90
Clutched-spring moment arm (mm)	32.1
Total orthosis mass (kg)	1.9

Joint powers were computed as the product of joint moments and joint velocities from SIMM-derived joint kinematics, where positive power was defined as that produced by the joint on the environment. Positive joint work during late stance knee flexion was computed as the positive contribution of the time-integral of joint power from maximum stance knee extension to toe-off. This region of the gait cycle was chosen for analysis because, as the knee flexes from the maximum extension angle, it provides an opportunity for the AG to provide positive power to the wearer. Joint flexion moment impulse was computed using the same integral for joint flexion moment. Net prosthesis work was computed by integrating the SIMM-derived joint torque over joint angle for the entire gait cycle.

Metabolic cost for each walking speed was computed by taking average oxygen and carbon dioxide data over a two-minute window at the end of each six-minute trial. The metabolic power was computed using the equation

$$P = K_{O_2}\dot{V}_{O_2} + K_{CO_2}\dot{V}_{CO_2}, \quad (4)$$

where P is the metabolic power in Watts, $\dot{V}_{O_2}$ is the volume flow rate of oxygen inhaled, $\dot{V}_{CO_2}$ is the volume flow rate of carbon dioxide exhaled, and K_{O_2} and K_{CO_2} are constants with values from literature [37], given as K_{O_2} = 16,580 W/L and K_{CO_2} = 4,510 W/L. The above equation is only valid for conditions when the metabolism is primarily aerobic. As a verification of this condition, the respiratory exchange ratio (RER), defined as $\dot{V}_{CO_2}/\dot{V}_{O_2}$, was monitored, and only metabolic results with RER values less than 1.1 were considered.

3. Results

3.1. Mechanical Design. The mechanical parameters of the design are summarized in Table 3. As in previous work [29], the teeth were manufactured using a contour milling process, and thus, the tooth spacing was limited by the 0.4 mm radius of the mills. Therefore, the tooth spacing was constrained to 4 degrees, or 90 teeth per revolution. The total mass of the orthosis, including battery and electronics, was 1.9 kg.

The aluminum teeth used in this design do not yield for applied knee flexion moments near to the expected values of 25 Nm [38] but start to yield at 35 times this expected load

Table 4: Net work per step by the powered ankle-foot prosthesis with the AG. The net work values were kept within the literature range of 0.045 to 0.16 J/kg.

	Baseline (J/kg)	Active (J/kg)
Subject 1	0.113 ± 0.028	0.130 ± 0.024
Subject 2	0.077 ± 0.016	0.082 ± 0.019

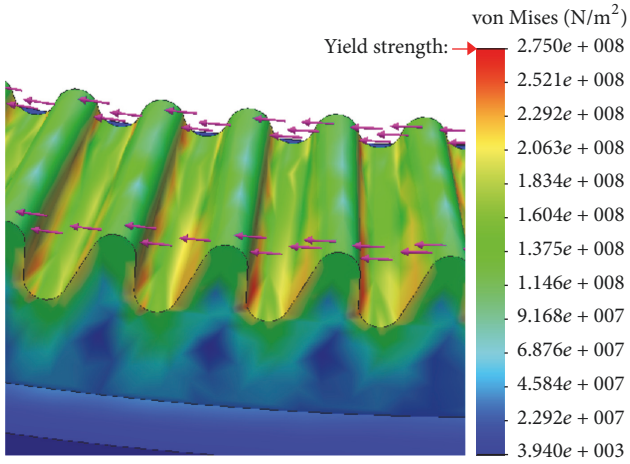

Figure 5: Results of finite element analysis with load evenly applied to all tooth tips tangentially. Results are shown for the yield condition, at which the applied torque to the clutch is 890 Nm.

(Table 3). The tooth stress at this failure load condition is shown in Figure 5.

3.2. Power Consumption. Given the solenoid specifications (22.2 V, 109 Ohms resistance), the power draw was 4.9 W. Assuming the maximum clutch-on time for each gait cycle of 0.4 ms and a typical cadence of 0.9 strides per second, the power consumption of the solenoid was 2.2 W. With the 1.1 W power draw of the Raspberry Pi, the average total power consumption of the device was 3.3 W during a typical walking gait.

3.3. Joint Spring Selection. The spring stiffness of the clutched-spring gastrocnemius element, derived from the modeling, was 92.9 Nm/rad [35]. To approximate this rotary stiffness about the knee joint, the two tangential linear compression springs were selected with spring constants of 51 N/mm. These springs acted on the joint with a moment arm of 32.1 mm, causing the equivalent joint rotary stiffness to be 105 Nm/rad.

3.4. Clinical Pilot Results

3.4.1. Acclimatization. In the time allotted for acclimatization, participants could walk with the AG and PAFP. Participants could walk comfortably with the AG, and the ankle prosthesis net work was appropriate for normal walking (see Table 4).

3.4.2. Ankle Prosthesis Net Work. As shown in Table 4, the net work produced by the powered ankle-foot prosthesis was within the desired range from literature [36].

3.4.3. Affected Knee Kinetics. Affected-side knee kinetics for both participants are shown in Figure 6 and summarized in Tables 5 and 6. Of particular note, the biological component of knee flexion moment impulse and the biological knee positive mechanical work during late stance knee flexion phase were both reduced by large percentage changes when subjects walked with the *Active* condition of the AG, compared to the *Baseline* condition.

3.4.4. Affected-Side Hip Kinetics. Hip flexion moment is shown in Figure 7, and hip flexion moment impulse values are summarized in Table 7. Hip net mechanical work values for both participants are shown in Table 8. As with the knee joint, both hip flexion moment impulse and positive mechanical work during late stance flexion were decreased slightly for both participants.

3.4.5. Metabolism. The net metabolic power (with the power required for standing subtracted out) is tabulated in Table 9. Both participants displayed small percentage reductions in metabolic cost when walking with the *Active* condition, as compared to the *Baseline* condition.

4. Discussion

Our novel design of a quasi-passive artificial gastrocnemius has been tested in our pilot study and found to be mechanically functional for the task of providing a flexion assist moment to the affected-side biological knee joint. The device exceeds the torque requirements while requiring only a small amount of electrical power. These properties make this a device a prime candidate for experiments for those with transtibial amputation, with the end goal of improving walking gaits for this population.

The preliminary findings from this study indicate that some measures of gait may be especially affected by the intervention. The pilot data support the hypothesis that this artificial gastrocnemius can reduce biological knee flexion moment and biological positive work of the affected-side knee, compared to a similarly weighted monoarticular prosthesis, during late stance knee flexion. Despite the short amount of time to get acclimated to the knee orthosis, the participants reduced their biological knee moment profiles, thereby allowing the AG to take over some of the kinetic loads. This behavior is consistent with other studies involving exoskeletal interventions at ankle [39] and hip joints [40]. The reduction of biological knee moment is beneficial from the standpoint of wearable device design, since it means that wearers of the AG were quickly able to replace biological function with that from the device.

Also as hypothesized, the affected-side hip flexion moment impulse and hip positive work of both participants were reduced during late stance knee flexion. These reductions are likely a result of the energy return of the spring, which served to help flex the hip. Although small, this effect

Table 5: Affected-side knee flexion moment impulse in late stance flexion with the AG compared between the two walking conditions with the quasi-passive artificial gastrocnemius: the Baseline condition, where the artificial gastrocnemius acted as a free-joint at the knee, and the Active condition, where the AG was appropriately engaged as per the controller. The values were computed over the late stance knee flexion phase of the gait cycle.

	Baseline moment impulse (Nm∗s/kg)	Active moment impulse (Nm∗s/kg)	Active Biological moment impulse (Nm∗s/kg)	Total % change from Baseline	Biological % change from Baseline
Subject 1	0.006 ± 0.004	0.009 ± 0.004	0.001 ± 0.002	+32	−78
Subject 2	0.055 ± 0.018	0.056 ± 0.013	0.039 ± 0.011	+2	−29

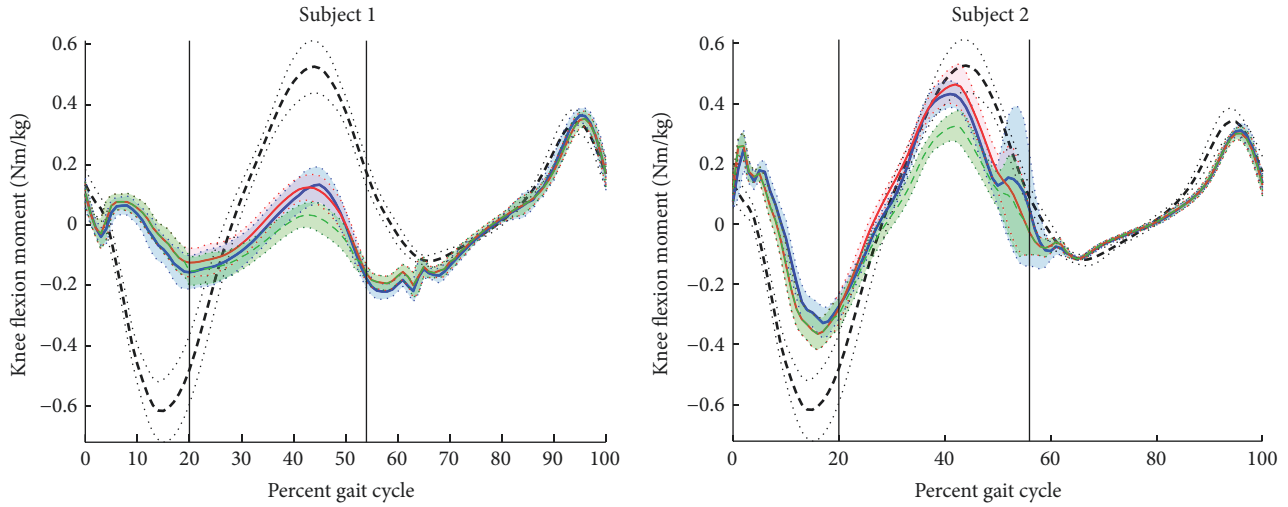

Figure 6: Affected-side knee flexion moment components with the AG shown for the *Baseline* condition where the clutch was disabled (thick solid blue line), the *Active* condition (thin solid red line), and the biological knee moment contribution during the *Active* condition (thin green dashed line). Shaded regions for these curves indicate ±1 standard deviation, bounded by light dotted lines. For reference, biological knee moment data are also shown for the nonamputee from which the clutch spring was tuned (thick black dashed line) ±1 standard deviation (black dotted lines). The vertical lines indicate the typical engagement and disengagement times for the clutch.

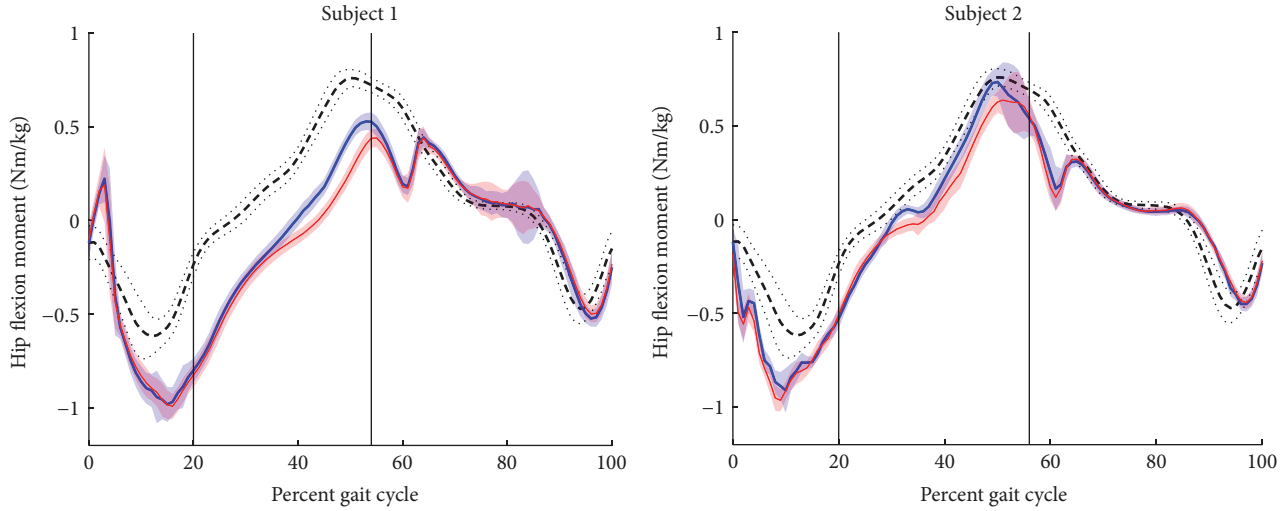

Figure 7: Affected-side hip flexion moment components with the AG shown for the *Baseline* condition where the clutch was disabled (thick solid blue line) and the *Active* condition (thin solid red line). Shaded regions for these curves indicate ±1 standard deviation. For reference, biological hip moment data are also shown for the nonamputee from which the clutch spring was tuned (thick black dashed line) ±1 standard deviation (black dotted lines). The vertical lines indicate the typical engagement and disengagement times for the clutch.

Table 6: Affected-side knee positive work in late stance flexion with the AG compared between the two walking conditions with the quasi-passive artificial gastrocnemius: the Baseline condition, where the artificial gastrocnemius acted as a free-joint at the knee, and the Active condition, where the AG was appropriately engaged as per the controller. The values were averaged over the late stance knee flexion phase of the gait cycle.

	Baseline total power (Nm∗s/kg)	Active total power (Nm∗s/kg)	Active biological power (Nm∗s/kg)	Total % change from Baseline	Biological % change from Baseline
Subject 1	0.006 ± 0.004	0.005 ± 0.003	0.002 ± 0.002	−6	−60
Subject 2	0.084 ± 0.064	0.062 ± 0.031	0.049 ± 0.030	−26	−41

Table 7: Hip flexion moment impulse in late stance flexion with the AG compared between the two walking conditions with the quasi-passive artificial gastrocnemius: the Baseline condition, where the artificial gastrocnemius acted as a free-joint at the knee, and the Active condition, where the AG was appropriately engaged as per the controller. The values were computed over the late stance knee flexion phase of the gait cycle.

	Baseline moment impulse (Nm∗s/kg)	Active moment impulse (Nm∗s/kg)	% change from Baseline
Subject 1	0.077 ± 0.006	0.057 ± 0.006	−26
Subject 2	0.134 ± 0.013	0.115 ± 0.012	−14

Table 8: Affected-side hip positive work in late stance flexion with the AG compared between the two walking conditions with the quasi-passive artificial gastrocnemius: the Baseline condition, where the artificial gastrocnemius acted as a free-joint at the knee, and the Active condition, where the AG was appropriately engaged as per the controller. The values were computed over the late stance knee flexion phase of the gait cycle.

	Baseline positive work (J/kg)	Active positive work (J/kg)	% change from Baseline
Subject 1	0.087 ± 0.011	0.063 ± 0.0090	−27
Subject 2	0.117 ± 0.016	0.095 ± 0.014	−19

Table 9: Metabolic power of the amputee participants with the AG.

	Subject 1	Subject 2
Baseline power (W/kg)	3.80 ± 0.19	3.04 ± 0.11
Active power (W/kg)	3.61 ± 0.19	2.94 ± 0.08
Percent change	−5%	−3%

may possibly compensate for the otherwise increased hip power exhibited by transtibial amputees [4].

Given the kinetic results, it is not surprising that slight metabolic improvements were demonstrated as well. Reductions in net positive biological mechanical work should correspond to reductions in concentric muscle work, since passive tissues, by definition, cannot generate net positive work. This reduction in muscle work, in turn, would be expected to reduce metabolic cost [41, 42].

5. Conclusions and Future Work

Despite the advances of today's monoarticular transtibial prostheses, their limitations still manifest in pathological gaits. This study builds on the hypothesis that dominant pathologies are caused by a lack of biarticular gastrocnemius function. Our approach of restoring this biarticular component via an artificial gastrocnemius has shown preliminary but promising results toward the improvement of transtibial prosthesis efficacy.

The quasi-passive nature of this novel artificial gastrocnemius means that the design could exclude heavy components like large batteries and motors. Yet still, this device has the capability to produce biological-levels of knee moments for assisting those with transtibial amputation. The low power draw also helps to make this device practical for daily use, as battery life would not likely be a problem over the course of a day.

The AG, despite lacking an ability to generate positive net mechanical work, did demonstrate an ability to reduce amputee metabolic cost of transport for the two amputees tested. This preliminary result suggests that biarticular devices may hold the potential to improve amputee quality of life beyond that with even the most advanced monoarticular devices. These metabolic benefits may stem from a combination of a reduction in knee and hip moments and powers in the affected-side leg.

However, given the lack of statistical power, more work is needed to verify this effect on more participants. In addition, the slight increase seen in the net mechanical work from the ankle-foot prosthesis during the ACTIVE conditions could

account for a nonnegligible portion of this small metabolic benefit. If, however, the metabolic improvement is confirmed for other amputees when ensuring no increase in positive work from the prosthetic ankle, it would show that metabolic improvements are possible for transtibial amputees without the need for the injection of net positive mechanical work.

It would be beneficial to perform additional experiments that more broadly explore this device. Each individual has their own gait idiosyncrasies, and a matching to other human gait solely based on height and weight has its limitations. Therefore, it is possible that, although the joint stiffness of the device was chosen via optimization, this stiffness value may not have corresponded to the optimal values for the given amputee participants. Additionally, inherent compliance in the brace itself may change the effective device stiffness from the designed specification. Future trials could more systematically vary the joint stiffness to find the metabolically optimal value and then compare it to that from simulation.

In addition, it may be desirable to reach beyond the quasi-passive model of the gastrocnemius muscle. Seeing that the biological gastrocnemius generates several joules of net work per step [43, 44], greater benefits could possibly be achieved by providing this net work to amputees. By definition, this net mechanical work cannot be produced with a quasi-passive device, and, therefore, a different mechanism would be needed to test this hypothesis. In the design of either quasi-passive or active transtibial leg prostheses, we feel biarticular gastrocnemius actuation is an important consideration.

Conflicts of Interest

The authors declare that there are no conflicts of interest regarding the publication of this article.

Acknowledgments

This work was supported by departmental funding in the MIT Media Lab.

References

[1] P. A. Struyf, C. M. van Heugten, M. W. Hitters, and R. J. Smeets, "The Prevalence of Osteoarthritis of the Intact Hip and Knee Among Traumatic Leg Amputees," *Archives of Physical Medicine and Rehabilitation*, vol. 90, no. 3, pp. 440–446, 2009.

[2] R. Gailey, K. Allen, J. Castles, J. Kucharik, and M. Roeder, "Review of secondary physical conditions associated with lower-limb amputation and long-term prosthesis use," *Journal of Rehabilitation Research and Development*, vol. 45, no. 1, pp. 15–29, 2008.

[3] D. M. Ehde, J. M. Czerniecki, D. G. Smith et al., "Chronic phantom sensations, phantom pain, residual limb pain, and other regional pain after lower limb amputation," *Archives of Physical Medicine and Rehabilitation*, vol. 81, no. 8, pp. 1039–1044, 2000.

[4] P.-F. Su, S. A. Gard, R. D. Lipschutz, and T. A. Kuiken, "Gait characteristics of persons with bilateral transtibial amputations," *Journal of Rehabilitation Research and Development* , vol. 44, no. 4, pp. 491–501, 2007.

[5] D. A. Winter and S. E. Sienko, "Biomechanics of below-knee amputee gait," *Journal of Biomechanics*, vol. 21, no. 5, pp. 361–367, 1988.

[6] N. H. Molen, "Energy/speed relation of below-knee amputees walking on a motor-driven treadmill," *Internationale Zeitschrift für Angewandte Physiologie Einschließlich Arbeitsphysiologie*, vol. 31, no. 3, pp. 173–185, 1973.

[7] R. L. Waters, J. Perry, D. Antonelli, and H. Hislop, "Energy cost of walking of amputees: the influence of level of amputation," *The Journal of Bone & Joint Surgery*, vol. 58, no. 1, pp. 42–46, 1976.

[8] J. Hu and R. G. Gordon, "Textured aluminum-doped zinc oxide thin films from atmospheric pressure chemical-vapor deposition," *Journal of Applied Physics*, vol. 71, no. 2, p. 880, 1992.

[9] H. M. Herr and A. M. Grabowski, "Bionic ankle-foot prosthesis normalizes walking gait for persons with leg amputation," *Proceedings of the Royal Society B Biological Science*, vol. 279, no. 1728, pp. 457–464, 2012.

[10] D. Hill and H. Herr, "Effects of a powered ankle-foot prosthesis on kinetic loading of the contralateral limb: a case series," in *Proceedings of the IEEE International Conference on Rehabilitation Robotics (ICORR '13)*, vol. 10, pp. 1–6, IEEE, Seattle, WA, USA, June 2013.

[11] C. H. Soo and J. M. Donelan, "Mechanics and energetics of step-to-step transitions isolated from human walking," *Journal of Experimental Biology*, vol. 213, no. Pt 24, pp. 4265–4271, 2010.

[12] A. D. Kuo, J. M. Donelan, and A. Ruina, "Energetic consequences of walking like an inverted pendulum: step-to-step transitions," *Exercise and Sport Sciences Reviews*, vol. 33, no. 2, pp. 88–97, 2005.

[13] J. M. Donelan, R. Kram, and A. D. Kuo, "Mechanical work for step-to-step transitions is a major determinant of the metabolic cost of human walking," *Journal of Experimental Biology*, vol. 205, no. 23, pp. 3717–3727, 2002.

[14] A. D. Kuo, "Energetics of actively powered locomotion using the simplest walking model," *Journal of Biomechanical Engineering*, vol. 124, no. 1, pp. 113–120, 2002.

[15] M. Meinders, A. Gitter, and J. M. Czerniecki, "The role of ankle plantar flexor muscle work during walking," *Journal of rehabilitation medicine*, vol. 30, no. 1, pp. 39–46, 1998.

[16] R. R. Neptune, S. A. Kautz, and F. E. Zajac, "Contributions of the individual ankle plantar flexors to support, forward progression and swing initiation during walking," *Journal of Biomechanics*, vol. 34, no. 11, pp. 1387–1398, 2001.

[17] A. L. Hof, J. Nauta, E. R. van der Knaap, M. A. A. Schallig, and D. P. Struwe, "Calf muscle work and segment energy changes in human treadmill walking," *Journal of Electromyography & Kinesiology*, vol. 2, no. 4, pp. 203–216, 1993.

[18] J. M. Caputo and S. H. Collins, "Prosthetic ankle push-off work reduces metabolic rate but not collision work in non-amputee walking," *Scientific Reports*, vol. 4, article no. 7213, 2014.

[19] M. R. Williams, A. Grabowski, H. Herr, and S. D'Andrea, *Electromyographic Effects of Using a Powered Ankle-Foot Prosthesis*, American Society of Biomechanics, 2012.

[20] J. F. Veneman, R. Kruidhof, E. E. G. Hekman, R. Ekkelenkamp, E. H. F. Van Asseldonk, and H. van der Kooij, "Design and Evaluation of the Gait Rehabilitation Robot LOPES," *IEEE Transactions on Neural Systems and Rehabilitation Engineering*, vol. 15, no. 3, 2007.

[21] J. E. Pratt, B. T. Krupp, C. J. Morse, and S. H. Collins, "The RoboKnee: an exoskeleton for enhancing strength and endurance during walking," in *Proceedings of the IEEE International Conference on Robotics and Automation (ICRA '04)*, vol. 3, pp. 2430–2435, IEEE, May 2004.

[22] P. P. Pott, S. I. Wolf, J. Block et al., "Knee-ankle-foot orthosis with powered knee for support in the elderly," *Proceedings of the Institution of Mechanical Engineers, Part H: Journal of Engineering in Medicine*, vol. 231, no. 8, pp. 715–727, 2017.

[23] D. P. Ferris, J. M. Czerniecki, and B. Hannaford, "An ankle-foot orthosis powered by artificial pneumatic muscles," *Journal of Applied Biomechanics*, vol. 21, no. 2, pp. 189–197, 2005.

[24] G. S. Sawicki and D. P. Ferris, "A pneumatically powered knee-ankle-foot orthosis (KAFO) with myoelectric activation and inhibition," *Journal of NeuroEngineering and Rehabilitation*, vol. 6, no. 1, p. 23, 2009.

[25] D. P. Ferris, K. E. Gordon, G. S. Sawicki, and A. Peethambaran, "An improved powered ankle-foot orthosis using proportional myoelectric control," *Gait & Posture*, vol. 23, no. 4, pp. 425–428, 2006.

[26] M. Wehner, B. Quinlivan, P. M. Aubin et al., "A lightweight soft exosuit for gait assistance," in *Proceedings of the IEEE International Conference on Robotics and Automation (ICRA '13)*, pp. 3362–3369, May 2013.

[27] M. B. Wiggin, G. S. Sawicki, and S. H. Collins, "An exoskeleton using controlled energy storage and release to aid ankle propulsion," in *Proceedings of the IEEE International Conference on Rehabilitation Robotics (ICORR '11)*, pp. 1–5, Zurich, Switzerland, June 2011.

[28] C. J. Walsh, K. Endo, and H. Herr, "A quasi-passive leg exoskeleton for load-carrying augmentation," *International Journal of Humanoid Robotics*, vol. 4, no. 3, pp. 487–506, 2007.

[29] G. Elliott, A. Marecki, and H. Herr, "Design of a clutch-spring knee exoskeleton for running," *Journal of Medical Devices, Transactions of the ASME*, vol. 8, no. 3, Article ID 031002, 11 pages, 2014.

[30] M. S. Cherry, D. J. Choi, K. J. Deng, S. Kota, and D. P. Ferris, "Design and Fabrication of an Elastic Knee Orthosis: Preliminary Results," in *Proceedings of the ASME 2006 International Design Engineering Technical Conferences and Computers and Information in Engineering Conference*, pp. 565–573, Philadelphia, PA, USA, 2006.

[31] M. Ishikawa, P. V. Komi, M. J. Grey, V. Lepola, and G.-P. Bruggemann, "Muscle-tendon interaction and elastic energy usage in human walking," *Journal of Applied Physiology*, vol. 99, no. 2, pp. 603–608, 2005.

[32] K. Endo and H. Herr, "A model of muscle-tendon function in human walking," in *Proceedings of the 2009 IEEE International Conference on Robotics and Automation, ICRA '09*, pp. 1909–1915, IEEE, Kobe, Japan, May 2009.

[33] K. Endo and H. Herr, "Human walking model predicts joint mechanics, electromyography and mechanical economy," in *Proceedings of the 2009 IEEE/RSJ International Conference on Intelligent Robots and Systems, IROS 2009*, pp. 4663–4668, St. Louis, MO, USA, October 2009.

[34] K. Endo, D. Paluska, and H. Herr, "A quasi-passive model of human leg function in level-ground walking," in *Proceedings of the 2006 IEEE/RSJ International Conference on Intelligent Robots and Systems, IROS 2006*, pp. 4935–4939, Beijing, China, October 2006.

[35] K. Endo, E. Swart, and H. Herr, "An artificial gastrocnemius for a transtibial prosthesis," in *Proceedings of the 31st Annual International Conference of the IEEE Engineering in Medicine and Biology Society: Engineering the Future of Biomedicine, EMBC 2009*, pp. 5034–5037, Minneapolis, MN, USA, September 2009.

[36] M. Palmer, *Sagittal Plane Characterization of Normal Human Ankle Function Across a Range of Walking Gait Speeds , Masters Thesis [Masters, thesis]*, MIT, 2002.

[37] J. M. Brockway, "Derivation of formulae used to calculate energy expenditure in man," *Hum Nutr Clin Nutr*, vol. 41, no. 6, pp. 463–471, 1987.

[38] A. S. McIntosh, K. T. Beatty, L. N. Dwan, and D. R. Vickers, "Gait dynamics on an inclined walkway," *Journal of Biomechanics*, vol. 39, no. 13, pp. 2491–2502, 2006.

[39] P.-C. Kao, C. L. Lewis, and D. P. Ferris, "Invariant ankle moment patterns when walking with and without a robotic ankle exoskeleton," *Journal of Biomechanics*, vol. 43, no. 2, pp. 203–209, 2010.

[40] C. L. Lewis and D. P. Ferris, "Erratum to "Invariant hip moment pattern while walking with a robotic hip exoskeleton" [J. Biomech. 44 (5) (2011) 789-793]," *Journal of Biomechanics*, vol. 47, no. 7, p. 1748, 2014.

[41] A. Hill, "The heat of shortening and the dynamic constants of muscle," *Proceedings of the Royal Society B*, vol. 126, pp. 136–195, 1938.

[42] A. Hill, "The efficiency of mechanical power development during muscular shortening and its relation to load," *Proceedings of the Royal Society B Biological Science*, vol. 159, no. 975, pp. 319–324, 1964.

[43] R. J. Zmitrewicz, R. R. Neptune, and K. Sasaki, "Mechanical energetic contributions from individual muscles and elastic prosthetic feet during symmetric unilateral transtibial amputee walking: A theoretical study," *Journal of Biomechanics*, vol. 40, no. 8, pp. 1824–1831, 2007.

[44] R. R. Neptune, K. Sasaki, and S. A. Kautz, "The effect of walking speed on muscle function and mechanical energetics," *Gait & Posture*, vol. 28, no. 1, pp. 135–143, 2008.